Kinetics and Catalysis, Vol. 41, No. 1, 2000, pp. 116–121. Translated from Kinetika i Kataliz, Vol. 41, No. 1, 2000, pp. 131–136.

Study of the Mobility of Lattice Oxygen in Complex Oxide Catalysts for Partial Oxidation of Propylene to Acrolein

A. A. Firsova, Yu. V. Maksimov, V. Yu. Bychkov, O. V. Isaev, I. P. Suzdalev, and V. N. Korchak

Semenov Institute of Chemical Physics, Russian Academy of Sciences, Moscow, Russia

Received March 10, 1998

Abstract—The amount of oxygen in the lattice of solids that participates in the elementary stages of partial propylene oxidation is determined for two types of Co–Mo–Bi–Fe–Sb–K–O catalysts (I, II) differing in the method of introduction of antimony and potassium. Two independent methods are used: (1) on the basis of the yield of the oxygen-containing products of propylene oxidation by oxygen of the catalyst in a pulse regime and (2) with the use of Möessbauer spectroscopy. Coincidence of the results obtained by both methods indicates that the active oxygen of the catalyst lattice is formed during redox transformations of iron(III) molybdate entering the composition of the catalysts. Data on the reduction of the catalysts in a pulse regime at various temperatures, which were processed in the framework of the diffusion model, allowed the estimation of the rate constants for diffusion of the lattice oxygen. An increase in the mobility of the lattice oxygen in catalyst I, which is modified with a small amount of antimony as compared to catalyst II, results in an increase in the overall productivity of the sample and in a decrease in the selectivity of propylene oxidation to acrolein. This correlates with the increase in the total amount of the lattice oxygen participating in the process.

INTRODUCTION

Previous study of the selective oxidation of olefins over multicomponent oxide catalysts containing Co, Bi, Fe, and other molybdates has shown that the oxygen of lattice O_L is involved in the formation of the reaction products [1–4]. The data of structural studies give evidence that the active reaction zone over a multicomponent catalyst is formed at the interfaces of various molybdates and the centers of the activation of olefin and oxygen are spatially separated [2, 3]. The active oxygen O_L that is consumed at the elementary stages of catalysis is evolved from iron(III) molybdate (IM) and reaches the reaction zone at the boundary of the crystallites of bismuth and iron molybdates by diffusion along the catalyst.

To enhance the catalytic activity and selectivity with respect to acrolein, the modifying additives such as antimony, potassium, and other compounds were introduced in multicomponent catalysts [5, 6]. The study of the effect of the catalyst composition on the structural features of IM and the diffusion mobility of the lattice oxygen is an important but still insufficiently understood problem.

The goal of this work is to determine the mobility of the lattice oxygen for two samples of the Co–Mo–Bi–Fe–Sb–K–O-containing catalysts for partial propylene oxidation, which differ by the method of preparation, and to study the effect of this mobility on the activity of the catalysts and the process selectivity. The absolute amount of O_L was estimated from the yield of oxygen-containing products of propylene oxidation by oxygen of the catalyst in a pulse regime and by Möessbauer spectroscopy. The rate constants for the diffusion of the lattice oxygen at various temperatures were estimated in the context of the diffusion model.

EXPERIMENTAL

Preparation of catalysts. The catalysts of the $Co_8Mo_{12}Bi_{0.75}Fe_3Sb_{0.3}K_{0.3}O_m$ ($m \sim 40$–50) composition were prepared by coprecipitation from solutions of ammonium paramolybdate, Co, Bi, and Fe nitrates and a combined salt and potassium-antimony tartrate. The potassium-antimony tartrate was introduced by two method. For the preparation of catalyst I, a portion of iron nitrate was added to a solution of the combined tartrate to obtain a precipitate containing antimony and iron. The slurry was then stirred and poured into a solution of ammonium paramolybdate to which an aqueous solution of cobalt and bismuth nitrates and the rest of the portion of iron nitrate were added. To prepare catalyst II, aqueous solutions of ammonium paramolybdate and cobalt, bismuth, iron nitrates, and the mixed salt of antimony and potassium tartrates were mixed together. The precipitates formed in both cases were dried at 120–130°C, calcined at 320–350°C until nitrates were completely decomposed, mixed with a necessary amount of aerosil 175 (7.5 wt %), granulated, and calcined again at 480°C for 5 h.

The methods of studying. Two methods were used for measuring the amount of the lattice oxygen participating in hydrocarbon oxidation. In the first method,

0023-1584/00/4101-0116$25.00 © 2000 MAIK "Nauka/Interperiodica"

propylene oxidation by the oxygen of a catalyst (reduction of a catalyst) was carried out in a microcatalytic reactor at 310, 340, and 370°C. The pulses of propylene (0.2 ml) were fed into the reactor with a dozing valve. A weighed portion of the catalyst was 0.5 g. A carrier-gas (helium) was thoroughly purified from traces of oxygen (up to 2×10^{-6} vol % O_2) by passing through a column with a chromia-silic adsorbent. The rate of the He flow was 50 ml/min, the duration between pulses was 5 min. The reaction products were analyzed by GC on columns packed with molecular sieve 5 Å and Porapak QS. The material balance with respect to carbon was made with an accuracy of 5–7%. In another method, the amount of the active lattice oxygen was determined by Möessbauer spectroscopy. The Möessbauer spectra were recorded with an instrument of the electrodynamic type with the source of ^{57}Co in chromium. The isomeric shifts (IS) were measured with respect to α-Fe. The spectra were processed with standard programs assuming the Lorentz line shape [7].

The catalytic activity was measured on a flow setup in the temperature range of 290–350°C at atmospheric pressure. The catalyst loading was 5 g, the time of contact was 4.2 s. The reaction mixture contained 5 vol % of propylene in air. The reaction products were analyzed by GC.

X-ray diffraction patterns were recorded on a DRON-3M instrument with filtered CuK_α radiation. Phases were identified by comparing the interplane distances with the known in published data [8].

The specific surface area of the samples was determined from the low-temperature adsorption of argon.

RESULTS AND DISCUSSION

The catalytic activity and selectivity with respect to the main reaction products for catalysts I and II measured in a flow reactor are presented in Table 1. (It should be noted that all data for the catalysts prepared many times by both methods are reproducible.) The propylene conversion on both catalysts is practically the same, equal to ~95% at 290°C, and increases to ~99% at 350°C. The selectivity with respect to acrolein over catalyst I is lower than that over catalyst II in the whole temperature range, and this difference is especially pronounced at 350°C (55 and 72%, respectively). The selectivities to acrylic and acetic acids are low over both catalysts.

Acrolein and water are the main products of the interaction of propylene with the oxygen of catalyst I in the pulse regime. The formation of CO_2 and acetic aldehyde was observed in the first 3–4 pulses. Only acrolein and water are formed during propylene oxidation over catalyst II in the pulse regime.

Figure 1 shows the data on the propylene conversion over both catalysts at 310, 340, and 370°C measured during 15 successive pulses. As can be seen, an overall trend to decreasing conversion with the number of

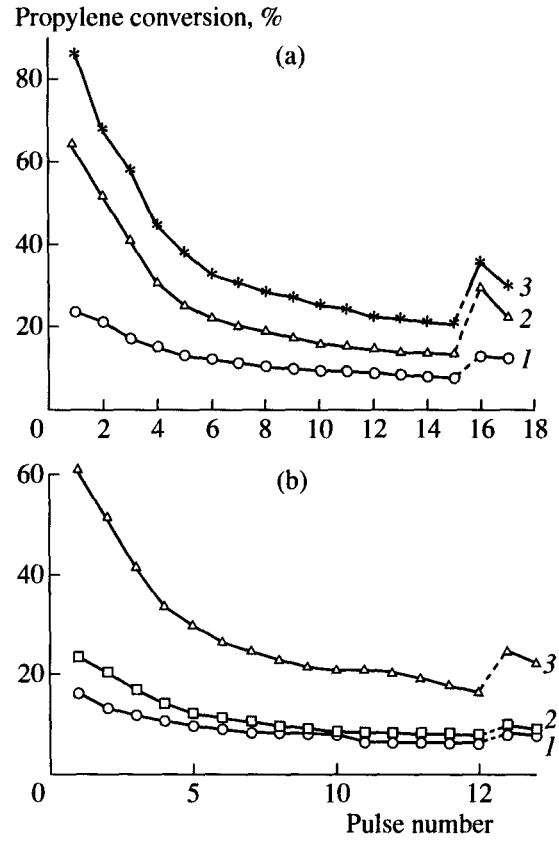

Fig. 1. Propylene conversion at (*1*) 310, (*2*) 340, and (*3*) 370°C in each of 17 successive pulses during reduction of catalysts I (a) and II (b).

pulses was observed. However, catalyst I exhibited higher activity than catalyst II. For instance, the propylene conversion over catalyst I in the first pulse at 310, 340, and 370°C was 25, 83, and 90% at the selectivity to acrolein of 100, 63, and 75%, respectively. The selectivity reached 100% after the fourth pulse at 340 and 370°C. The initial conversion in the first pulse over catalyst II at 310, 340, and 370°C was 16, 23, and 73%, and the selectivity to acrolein was 100, 100, and 85%, respectively. The selectivity increased to 100% after the fourth pulse of propylene at 370°C.

The diffusion of lattice oxygen from the bulk of the catalyst toward its surface was studied on the basis of a "repose" effect. After 15 successive pulses of propylene, the catalyst was kept at the temperature of the run under a helium atmosphere for 45 min, and then the propylene pulses were resumed (see Fig. 1, pulses 16 and 17). The propylene conversion over both samples after the "repose" increased by a factor of ~1.5 as compared to the 15th pulse. After reduction, a balance with respect to oxygen was calculated by summing the contributions of all oxygen-containing reaction products. The reduced catalysts were studied by Möessbauer spectroscopy to estimate the concentrations of the reduced species of iron molybdates.

Table 1. Propylene conversion and selectivity to main reaction products over catalysts I and II

Catalyst	T, °C	Conversion of C_3H_6, %	Selectivity, %				
			CH_2=CH–CHO	CO	CO_2	CH_3COOH	CH_2=CH–COOH
I	290	96.5	88.7	1.3	4.6	0.5	4.6
	310	98.1	83.5	2.2	6.6	0.7	6.9
	330	98.9	73.8	4.4	11.5	0.5	10.0
	350	99.0	55.0	11.2	21.4	0.2	12.0
II	290	94.4	92.8	0.6	2.4	0.2	4.2
	310	98.1	88.1	0.9	3.7	0.3	7.0
	330	98.3	83.6	1.4	5.2	0.2	9.2
	350	98.6	72.0	9.1	6.7	0.2	12.0

Table 2. Parameter r (see the text) and the amount of the lattice oxygen (O_L) removed from catalysts I and II during 17 pulses of propylene as studied by kinetics and Möessbauer spectroscopy

Catalyst	T, °C	$r = s(Fe^{2+})/s_{total}$	$[O_L] \times 10^4$, mol/g	
			reduction in a pulse regime	Möessbauer spectra
I	310	0.16	0.20	0.19
	340	0.29	0.38	0.36
	370	0.48	0.58	0.59
II	310	0.14	0.15	0.17
	340	0.21	0.24	0.26
	370	0.37	0.44	0.45

According to X-ray diffraction data, both catalysts are heterophase samples containing well-crystallized phases β-$CoMoO_4$, α-$Bi_2(MoO_4)_3$, and $Fe_2(MoO_4)_3$ with the average size of crystallites $\langle d \rangle \sim 180$–250 nm. Noteworthy is the fact that the formation of the antimony compounds in catalysts I and II was not observed.

Figure 2 presents the Möessbauer spectra of catalysts I and II in the original state (a, b), as well as the spectrum (c) typical of both catalysts after 17 pulses. The spectrum in Fig. 2a corresponds to two states of high-spin Fe^{3+} ions in the FeO_6 polyhedra with the values of the isomeric shift IS(1) = 0.42 ± 0.03 mm/s, quadrupole splitting $QS(1) = 0.45 \pm 0.03$ mm/s, the relative content $\delta(1) \approx 86\%$ and IS(2) = 0.43 ± 0.03 mm/s, $QS(2) = 0.19 \pm 0.03$ mm/s, and $\delta(2) \sim 14\%$. The parameters of state 2 are close to those of crystalline $Fe_2(MoO_4)_3$ [1], whereas the parameters of state I correspond to those of deformationally loaded $Fe_2(MoO_4)_3$ [9, 10]. The spectrum of catalyst II can be interpreted in a similar way with one difference: the parameters of the deformationally loaded iron species (IS(1) = 0.40 ± 0.03 mm/s, $QS(1) = 0.55 \pm 0.03$ mm/s, $\delta(1) \sim 92\%$) point to greater axial distortions of the local polyhedron FeO_6 than similar iron species in catalyst I. Thus, iron mainly exists in both catalysts in the form of the deformationally loaded species of iron(III) molybdate with various deviations from the cubic symmetry typical of stoichiometric $Fe_2(MoO_4)_3$.

A typical spectrum of catalysts I and II after 17 pulses of propylene is presented in Fig. 2c. Along with a doublet from $Fe_2(MoO_4)_3$, four new lines of equal intensity from two structurally nonequivalent positions of iron atoms (A, B) in the high-temperature modification of iron(II) molybdate β-$FeMoO_4$ with the parameters IS(A) = 1.08 ± 0.03 mm/s, $QS(A) = 1.12 \pm 0.03$ mm/s and IS(B) = 1.12 ± 0.03 mm/s, $QS(B) = 2.62 \pm 0.03$ mm/s are present in the spectrum. Notably, β-$FeMoO_4$ is isostructural to sheelite β-$CoMoO_4$ that is a basis for the catalysts under study, and hence it cannot be identified by X-ray diffraction.

The spectroscopic data not only testify to iron(III) molybdate reduction during interaction of the catalysts with propylene but also allow one to determine quantitatively the extent of reduction. Table 2 shows the parameter $r = s(Fe^{2+})/s_{tot}$, which is the ratio of the normalized area of the spectrum of iron(II) molybdate to the overall area of the spectrum. This parameter describes the extent of reduction of iron(III) molybdate and allows one to determine the quantity of active lattice oxygen O_L that participates in propylene oxidation according to the stoichiometry of reduction [1, 2]

$$Fe_2(MoO_4)_3 \longrightarrow 2\beta\text{-}FeMoO_4 + MoO_3 + O_L. \quad (I)$$

The estimates of the O_L value by two different methods are compared in Table 2: (1) from the amount of oxygenates formed during the reduction of the catalysts by propylene in the pulse regime and (2) by Möessbauer spectroscopy. As can be seen, the quantities of the evolved lattice oxygen O_L evaluated by two independent methods are practically the same. It follows from these data that reaction (I) plays a decisive role in supplying the active lattice oxygen to the reaction zone, where activation of propylene and its transformation occur. It is seen from Table 2 that the amount of O_L is different for catalysts I and II, which differ only by the method of introducing antimony.

An attempt to evaluate the effect of the antimony ion on the state of iron (III) molybdate in catalysts I and II can be made. It has been shown in [11] that the local properties of the iron ion in $Fe_2(MoO_4)_3$ in the FeO_6 polyhedron is sensitive to the Fe/Bi ratio. Taking into account that the isomeric shift of crystalline iron (III) molybdate is independent of the Fe/Bi ratio [11] and the quadrupole splitting is practically constant in the range of $T = 20$–350°C, one can conclude that deformations of the local polyhedron FeO_6 play the main role in

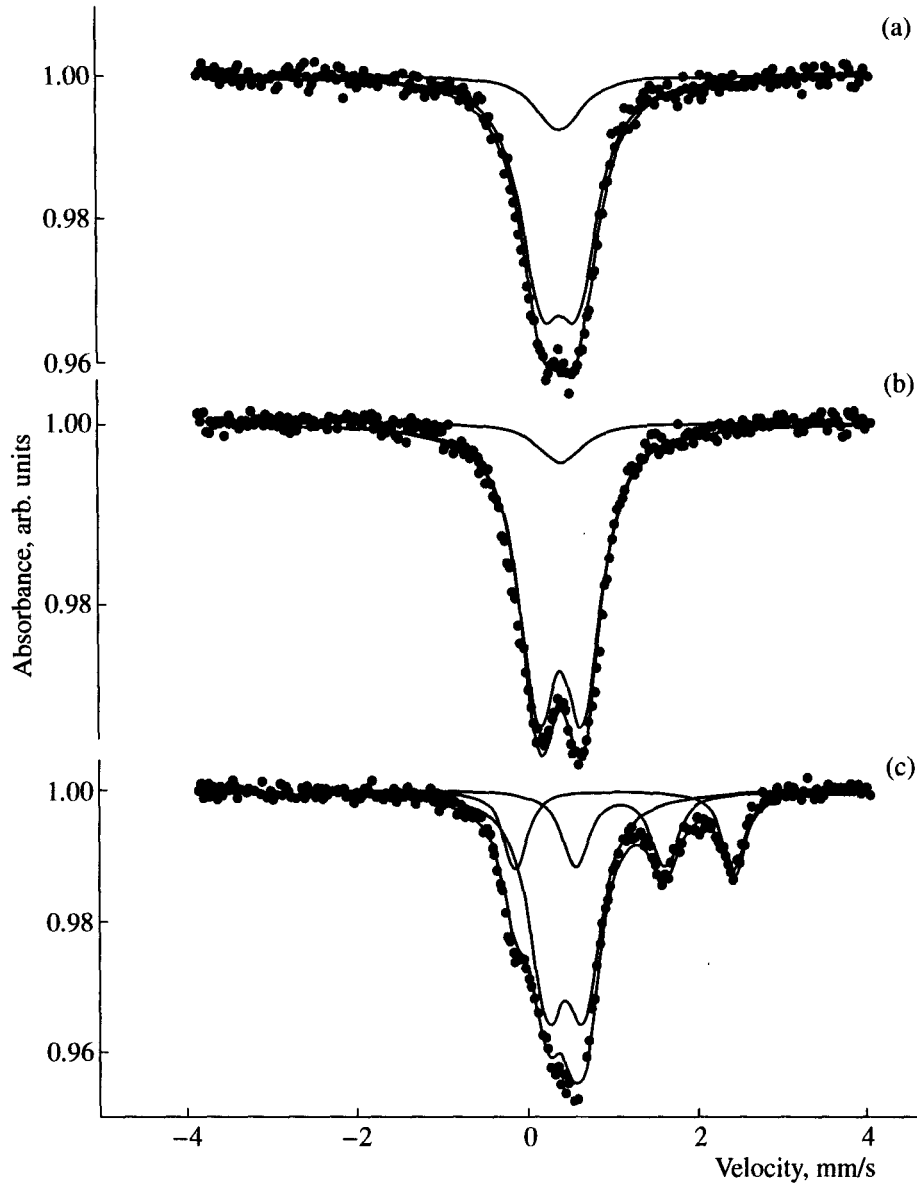

Fig. 2. Möessbauer spectra at room temperature of (a) catalyst I and (b) catalyst II in the initial state and (c) of catalyst II after reduction by 17 pulses of propylene at 370°C.

the variation of QS. The greater the Fe/Bi ratio, the smaller the deformations and the closer the parameters of Möessbauer spectra of iron (III) molybdate to those of a bulk single crystal [1]. One can suggest that in the catalyst, antimony and bismuth molybdate form solid solutions of substitution, $M_3FeMo_2O_{12}$ or $M_2Fe_2Mo_2O_{12}$, where M = Bi, Sb [3, 12]. In this case, the deformations in iron molybdate should be determined by the Fe/(Bi + Sb) ratio rather than by the Fe/Bi ratio. The QS value for the initial catalyst I is smaller than that for catalyst II; hence, the Fe/(Bi + Sb) ratio is greater for sample I than that for sample II. Since the amount of bismuth in both catalysts is the same, the amount of antimony entering the solid solution of substitution in catalyst I and thereby modifying its structure should be smaller than the corresponding amount for catalyst II. Hence, the differences in the activity of catalysts I and II and in the selectivity with respect to acrolein are due to different extents of modification of the bismuth molybdate lattice by antimony. These conclusions are true in the case when antimony does not form any separate compound that cannot be identified by X-ray diffraction.

It was taken into account in the development of the diffusion model that iron(III) molybdate is the phase containing the active lattice oxygen O_L that participates in propylene oxidation over catalysts I and II. The diffusion mobility of the lattice oxygen was estimated from the data on the "repose" of catalysts I and II during their reduction by propylene in the pulse regime. As

Table 3. The diffusivity of the lattice oxygen O_L (D) and the rate constants for propylene oxidation (k) measured during reduction of catalysts I and II by propylene in the pulse regime

Catalyst	T, °C	$D \times 10^{17}$, cm^2/s	k, l mol^{-1} s^{-1}
I	310	1.5	6.0
	340	6.0	2.3
	370	1.5	8.0
II	310	0.5	3.8
	340	1.0	6.0
	370	1.7	2.1

follows from Fig. 1, the propylene conversion in the 16th pulse, i.e., after the "repose", increased by 50–60% for both catalysts, and this effect is more pronounced for catalyst II. Hence, the active lattice oxygen participating in propylene oxidation arrived at the catalyst surface during the "repose" as a result of diffusion.

A sequence of the relatively fast processes such as adsorption, surface interactions, and desorption of the reaction products occur during the interaction between propylene and the surface of the multicomponent catalyst. The data available are insufficient for modeling all these stages, which are characterized by independent rate constants. Assuming that the complicated process of propylene oxidation to acrolein can be described by the overall reaction

$$C_3H_6 + 2O_L \longrightarrow C_3H_4O + H_2O, \quad \text{(II)}$$

the reaction rate can be approximated with sufficient accuracy as follows:

$$w = k[C_3H_6][O_L]. \quad (1)$$

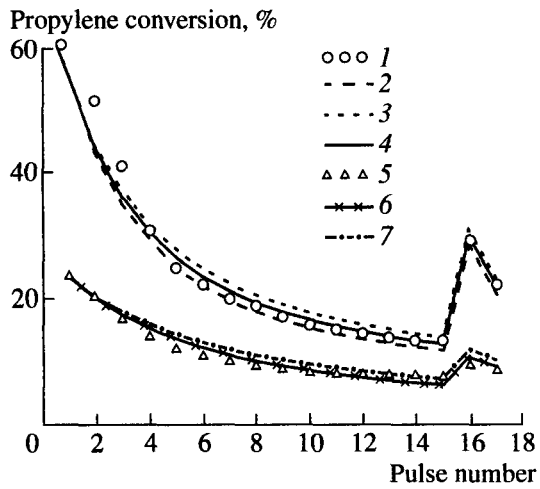

Fig. 3. Experimental (curves *1*, *5*) and calculated (curves *2–4*, *6*, *7*) data on the propylene conversion over catalysts I (*1–4*) and II (*5–7*) at the values of $D \times 10^{17}$: (*2*) 5, (*3*) 7, (*4*) 6, (*6*) 1.0, and (*7*) 1.5 cm^2/s, respectively. T = 340°C.

Here the order with respect to oxygen is 1 provided that the trimolecular reaction with the participation of two surface oxygen atoms is improbable and the hydrocarbon molecule reacts with one surface oxygen atom in real elementary stages:

$$C_3H_6 + O_L \longrightarrow C_3H_5O + H_s,\ H_s + O_L \longrightarrow OH_s \text{ etc.}$$

Since the average size of the crystallites of iron molybdate in the catalysts under study is equal to 180–250 nm, one can evaluate the surface area of iron molybdate, S_{im}, from its weight fraction. It was assumed in computer simulation that the crystallite of iron molybdate consists of the plates with the known thickness, the surface area of iron molybdate is close to S_{im}. Let us suggest that the active lattice oxygen O_L that directly interacts with propylene forms a layer with a depth of ~0.5 nm on the surface of iron molybdate. The anionic vacancies formed after the removal of O_L are filled by the lattice oxygen due to its diffusion from the bulk of the crystal. Then the change in the O_L concentration in each layer can be expressed as follows [6]

$$d[O_{L_i}] = 2D/h^2([O_{L_{i+1}}] - 2[O_{L_i}] + [O_{L_{i-1}}])dt, \quad (2)$$

where D is the diffusivity of the lattice oxygen in iron molybdate; h is the distance between the points in which the values $[O_{L_i}]$ ($h \sim 0.5$ nm); $[O_{L_i}]$, $[O_{L_{i+1}}]$, and $[O_{L_{i-1}}]$ are the concentrations of oxygen in the ith, $(i+1)$th, and $(i-1)$th layers, respectively.

Computer analysis of this model allowed us to calculate the propylene conversions in a series of successive pulses from the specified rate constants of oxidation k and the diffusion constants D chosen as parameters. Figure 3 presents the results of analysis. The most satisfactory coincidence of the experimental and calculated data is reached with the values of the k and D parameter shown in Table 3. The activation energy of propylene oxidation by oxygen of the catalyst as well as the activation energy for O_L diffusion in catalysts I and II were estimated to be 135 and 88 kJ/mol (catalyst I) and 120 and 154 kJ/mol (catalyst II), respectively.

Thus, one can conclude that the main source of the reactive oxygen during partial propylene oxidation over catalysts I and II is the crystal of iron(III) molybdate. The optimum mobility of the lattice oxygen is necessary to obtain the optimum ratio between the activity and selectivity of the catalyst. An increase in the mobility of the lattice oxygen in catalyst I results in a decrease in the selectivity of propylene oxidation. The diffusivity of the lattice oxygen is greater for catalyst I as compared to catalyst II. The selectivity of propylene oxidation matches the extent of deformation of the nanocrystal of iron(III) molybdate: the smaller the extent of axial distortions of the local FeO_6 polyhedron (catalyst I), the lower the selectivity. A higher mobility of the active oxygen O_L and a higher initial activity are observed in the case of the less distorted lattice of iron(III) molybdate in catalyst I as compared to catalyst II.

REFERENCES

1. Maksimov, Yu.V., Zurmukhtashvili, M.Sh., Suzdalev, I.P., *et al.*, *Kinet. Katal.*, 1984, vol. 25, no. 4, p. 948.
2. Krylov, O.V., Maksimov, Yu.V., and Margolis, L.Ya., *J. Catal.*, 1985, vol. 95, no. 1, p. 289.
3. Maksimov, Yu.V., Zurmukhtashvili, M.Sh., and Suzdalev, I.P., *Application of the Möessbauer Effect*, Kagan, Yu.M. and Lyubutin, I.S., Eds., Amsterdam: Gordon and Breach, 1985, vol. 3, p. 1051.
4. Firsova, A.A., Zurmukhtashvili, M.Sh., and Margolis, L.Ya., *Kinet. Katal.*, 1986, vol. 25, no. 5, p. 1208.
5. Maksimov, Yu.V., Firsova, A.A., Lubentsov, B.Z., and Shashkin, D.P., *Kinet. Katal.*, 1983, vol. 24, no. 2, p. 460.
6. Firsova, A.A., Vorob'eva, G.A., and Margolis, L.Ya., *Kinet. Katal.*, 1986, vol. 27, no. 5, p. 1213.
7. Maksimov, Yu.V., Suzdalev, I.P., Khomenko, T.I., and Kadushin, A.A., *Hyperfine Interaction*, 1990, vol. 57, p. 1987.
8. *ASTM, X-ray Powder Data File*, Smith, J.V., Ed., 1964.
9. Maksimov, Yu.V., Suzdalev, I.P., Engelmann, H., and Gonser, U., *Hyperfine Interaction*, 1986, vol. 27, p. 429.
10. Messinev, M.Yu., Maksimov, Yu.V., and Kushnerev, M.Ya., *Khim. Vys. Energ.*, 1979, vol. 13, no. 2, p. 377.
11. Zurmukhtashvili, M.Sh., Maksimov, Yu.V., Kutyrev, M.Yu., Margolis, L.Ya., Shashkin, D.P., and Krylov, O.V., *Kinet. Katal.*, 1984, vol. 25, no. 4, p. 955.
12. Shashkin, D.P., Maksimov, Yu.V., Shiryaev, P.A., and Matveev, V.V., *Kinet. Katal.*, 1991, vol. 32, no. 5, p. 1200.